Storm-driven mixing and potential impact on the Arctic Ocean

Jiayan Yang,[1] Josefino Comiso,[2] David Walsh,[3] Richard Krishfield,[4] and Susumu Honjo[4]

Received 5 December 2001; revised 18 June 2003; accepted 4 September 2003; published 9 April 2004.

[1] Observations of the ocean, atmosphere, and ice made by Ice-Ocean Environmental Buoys indicate that mixing events reaching the depth of the halocline have occurred in various regions in the Arctic Ocean. Our analysis suggests that these mixing events were mechanically forced by intense storms moving across the buoy sites. In this study, we analyzed these mixing events in the context of storm developments that occurred in the Beaufort Sea and in the general area just north of Fram Strait, two areas with quite different hydrographic structures. The Beaufort Sea is strongly influenced by inflow of Pacific water through Bering Strait, while the area north of Fram Strait is directly affected by the inflow of warm and salty North Atlantic water. Our analyses of the basin-wide evolution of the surface pressure and geostrophic wind fields indicate that the characteristics of the storms could be very different. The buoy-observed mixing occurred only in the spring and winter seasons when the stratification was relatively weak. This indicates the importance of stratification, although the mixing itself was mechanically driven. We also analyze the distribution of storms, both the long-term climatology and the patterns for each year in the past 2 decades. The frequency of storms is also shown to be correlated (but not strongly) to Arctic Oscillation indices. This study indicates that the formation of new ice that leads to brine rejection is unlikely the mechanism that results in the type of mixing that could overturn the halocline. On the other hand, synoptic-scale storms can force mixing deep enough to the halocline and thermocline layer. Despite a very stable stratification associated with the Arctic halocline, the warm subsurface thermocline water is not always insulated from the mixed layer. *INDEX TERMS:* 4207 Oceanography: General: Arctic and Antarctic oceanography; 4540 Oceanography: Physical: Ice mechanics and air/sea/ice exchange processes; 4572 Oceanography: Physical: Upper ocean processes; 4568 Oceanography: Physical: Turbulence, diffusion, and mixing processes; *KEYWORDS:* Arctic Ocean, mixing, storm, upper ocean

Citation: Yang, J., J. Comiso, D. Walsh, R. Krishfield, and S. Honjo (2004), Storm-driven mixing and potential impact on the Arctic Ocean, *J. Geophys. Res.*, *109*, C04008, doi:10.1029/2001JC001248.

1. Introduction

[2] There is some observational evidence to support the scenario that the Arctic climate system may have undergone considerable change in the past few decades [e.g., *Walsh et al.*, 1996; *Power and Mysak*, 1992; *Carmack et al.*, 1997; *Slonosky et al.*, 1997; *Parkinson et al.*, 1999; *Morison et al.*, 2000]. It is not yet clear whether these changes represent long-term trends or just phases of an oscillatory natural variability [e.g., *Mysak and Venegas*, 1998; *Thompson and Wallace*, 1999]. The best measured variable in the Arctic climate system over the past 2 decades is the sea ice concentration (SIC) from satellite passive microwave sensors. The SIC data reveal that the areal coverage of sea ice in the summer season has been decreasing by about 2.5% per decade since the advent of satellite-borne observations in the 1970s [*Parkinson et al.*, 1999]. The reduction in SIC has also appeared to accelerate since the early 1990s. Meanwhile, submarine observations also indicate that the sea ice may have been thinning. Taking these together, one may conclude that the total volume of Arctic sea ice has been shrinking, at least in recent decades. A more definite assessment can only be made when more observations become available.

[3] The change of total ice volume in the Arctic depends on several factors, including the export of sea ice to the Nordic Seas through Fram Strait and the local thermodynamics that govern the cycle of freezing and melting. Sea ice transport is determined largely by surface wind stress and oceanic current [e.g., *Thorndike and Colony*, 1982; *Colony and Thorndike*, 1984; *Proshutinsky and Johnson*, 1997]. The ice export to the Nordic Seas is correlated well with the North Atlantic Oscillation or the Arctic Oscillation [e.g., *Kwok*, 2000; *Kwok and Rothrock*, 1999] and has

[1]Department of Physical Oceanography, Woods Hole Oceanographic Institution, Woods Hole, Massachusetts, USA.
[2]Laboratory for Hydrospheric Processes, NASA Goddard Space Flight Center, Greenbelt, Maryland, USA.
[3]International Arctic Research Center, University of Alaska, Fairbanks, Fairbanks, Alaska, USA.
[4]Department of Geology and Geophysics, Woods Hole Oceanographic Institution, Woods Hole, Massachusetts, USA.

0148-0227/04/2001JC001248$09.00

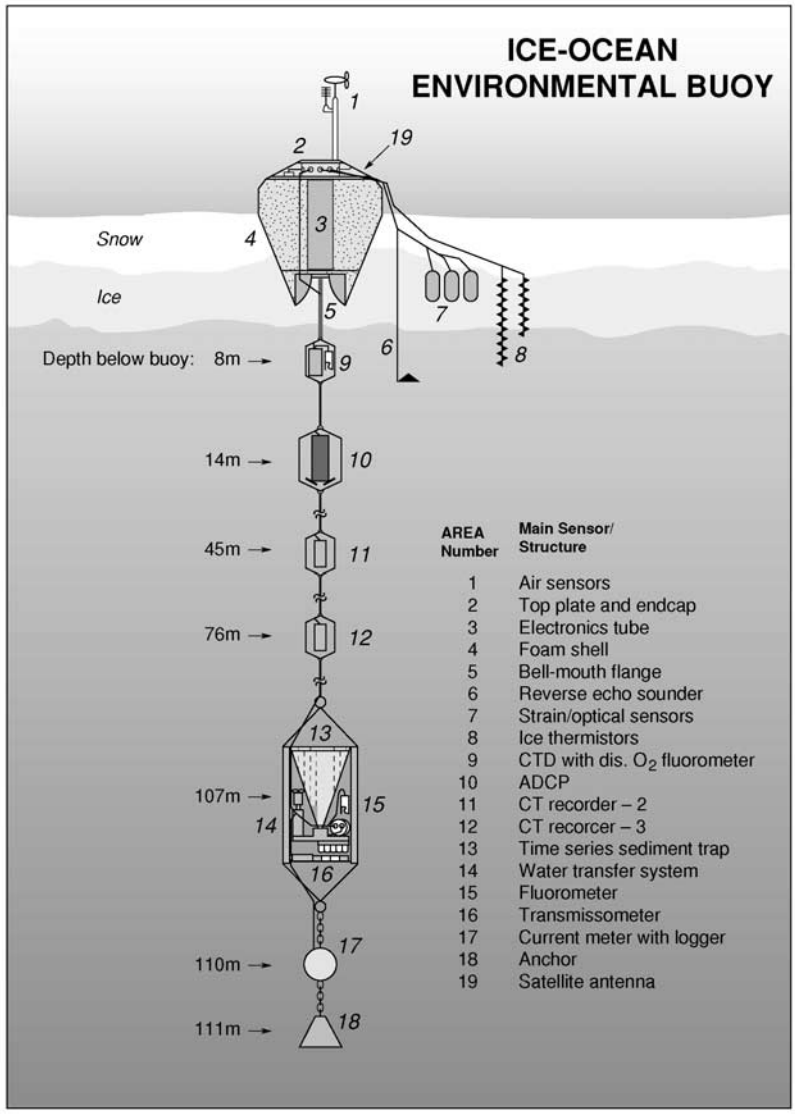

Figure 1. Schematic of the Ice-Ocean Environmental Buoy (IOEB). The IOEB buoys were deployed by the Woods Hole Oceanographic Institution (WHOI) and Japan Marine Science and Technology Center (JAMSTEC) in 1990s.

been shown to affect sea ice condition in Greenland and Labrador Seas [e.g., *Dickson et al.*, 1988; *Mysak et al.*, 1990]. The local thermodynamical balance can be affected by many processes. The solar radiation through open water areas in the summer season is a primary source of heat to the Arctic Ocean mixed layer [e.g., *Maykut and McPhee*, 1995]. Lateral advection within the mixed layer is less important, since the temperature is uniformly near the freezing point in all seasons. The subsurface layer of warm Atlantic water is an enormous reservoir of heat, but it is separated from the mixed layer by a stable Arctic halocline in the 30–50 m depth range [*Aagaard et al.*, 1981]. It is widely believed that convective mixing, even with brine rejection in winter, is not deep enough to reach the warmer thermocline water, so the heat flux from deeper layers is often considered to be small for the overall heat budget in the mixed layer. Such an assessment is based mainly on the consideration of buoyancy flux, such as brine rejection in winter. In this study we will show that intense storms could actually force mixing through the Arctic halocline to the thermocline.

[4] Brine rejection during the formation of sea ice is a mechanism which has received a great deal of attention in the study of mixing in the polar and subpolar oceans. It induces static instability, which is responsible for some types of deep mixing in high-latitude oceans, particularly in areas where the stratification is weak (such as the Labrador and Greenland Seas). This mechanism is less effective in the Arctic Ocean where the stratification near the surface is very stable. The deepening of the mixed layer can also be induced by an intense flux of kinetic energy, caused by enhanced air-sea or ice-water stress. This type of mixing has been observed in the Arctic Ocean. For instance, data collected by a SALARGOS buoy northeast of Svalbard showed that a storm in October 1988 intensified vertical mixing, enhanced the entrainment of warm and salty At-

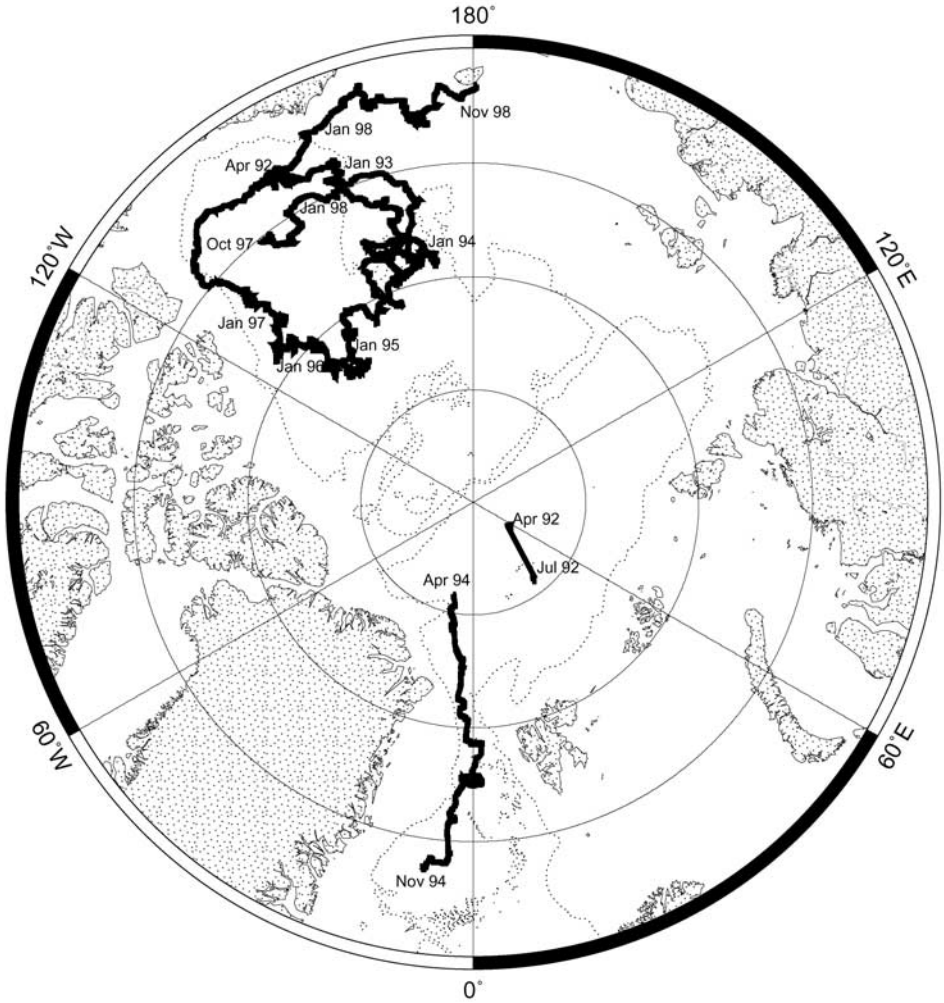

Figure 2. Drift tracks for all IOEBs from April 1992 through November 1998. The dotted line shows the 2000 m isobath.

lantic water into the mixed layer, and resulted in considerable melting of sea ice [*Steele and Morison*, 1993]. *Yang et al.* [2001], who analyzed oceanic, atmospheric, and sea ice data collected by a drifting buoy [*Honjo et al.*, 1995; *Krishfield et al.*, 1999], also reported mixing events in the Beaufort Sea. They attributed the mixing to intensive surface forcing associated with storms.

[5] In this study hydrographic data collected by the Ice-Ocean-Environmental Buoy (IOEB) [*Honjo et al.*, 1995; *Krishfield et al.*, 1999] are examined to identify mixing events reaching the halocline or deeper. We use atmospheric data from IOEBs, as well as from the International Arctic Buoy Program (IABP), and the NCEP-NCAR reanalyses to examine the development of wind and pressure fields during each mixing event. We also examine the characteristics of synoptic storms in the Arctic and their relationship to the longer timescale variations associated with the Arctic Oscillation.

2. Buoy and Satellite Data

[6] The IOEB was designed to acquire and transmit coherent, multivariable, environmental data while drifting in the Arctic pack ice through all seasons for several years [*Krishfield et al.*, 1993]. It was deployed jointly by the Woods Hole Oceanographic Institution (WHOI) and Japan Marine Science and Technology Center (JAMSTEC). The autonomous buoy system contained meteorological sensors measuring air temperature, pressure, wind velocity, ice temperature, as well as ocean sensors on a subice mooring system, including CT recorders, dissolved oxygen sensors, an Acoustic Doppler Current Profiler (ADCP), fluorometers, transmissometers, electromagnetic current meters, and a sediment trap. In all, the IOEB measured geophysical parameters over a range extending from the lower atmosphere just above the ice surface down through the ice column and into the upper ocean, as deep as the bottom of the Arctic halocline. Most instruments and sensors sampled at hourly intervals, and were tracked by Argos satellites. The buoy configuration is shown in Figure 1. Between 1992 and 1998 three buoys were deployed a total of six times in multiyear pack ice in the Arctic Ocean (see Figure 2 shows the buoy trajectories). The processing scheme for the telemetered data, as well as the individual IOEBs and field operations, are described in detail by *Krishfield et al.* [1993, 1999]. The buoy instrument con-

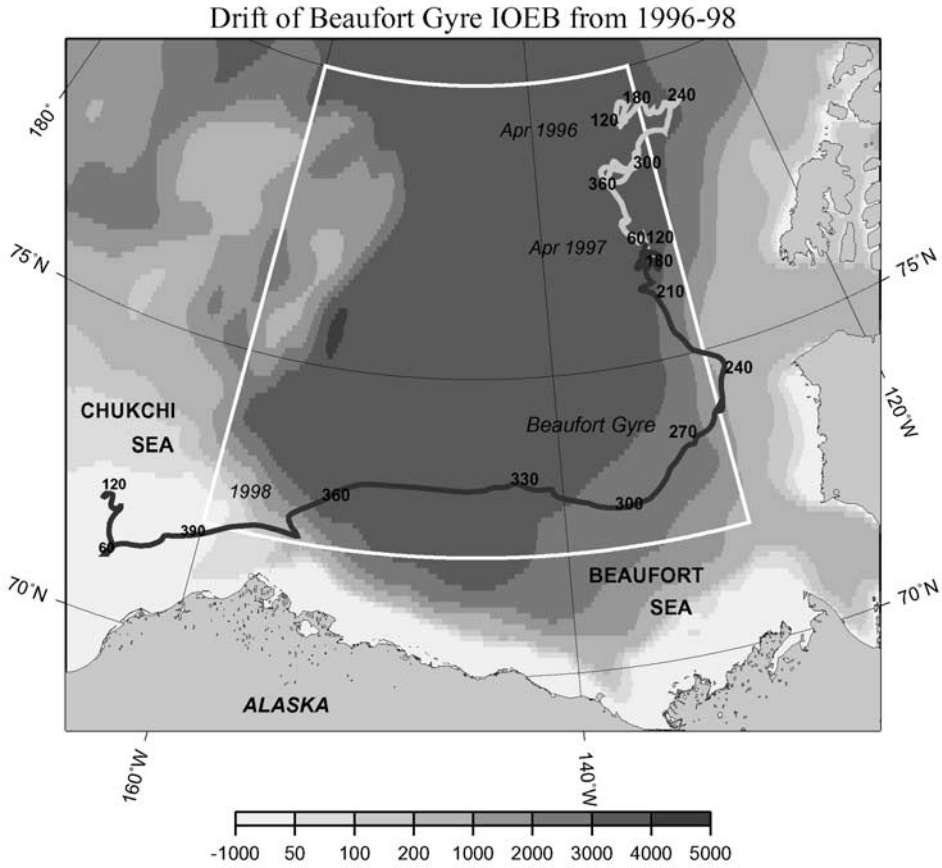

Figure 3. Trajectory of the Beaufort Sea buoy after being refurbished in April 1996, after which hydrographic measurements became available.

figurations were modified in each deployment. Our interest here is primarily in the hydrography and its variations. These data were available only for the periods between April and November 1994 in the transpolar region; and April 1996 to 1998 in the Beaufort Sea. The buoy was trapped in the shelf area in early 1998, and so we will use data prior to the end of 1997.

[7] In addition to meteorological data from the buoys, we also use sea level pressure (SLP) and surface and geostrophic winds from both NCEP-NCAR reanalyses [*Kalnay et al.*, 1996] and from the International Arctic Buoy Program (IABP) [*Thorndike and Colony*, 1980]. In addition, we use sea ice concentration observed by satellites to quantify the extent of sea ice, the total ice cover, and the amount of open water in the ice pack. Meteorological data is also used to partition fluxes of heat, fresh water and momentum in open water and ice-covered areas. Sea ice concentration data derived by using the bootstrap technique [*Comiso*, 1995] are also used.

[8] We have compared the IOEB SLP and surface winds with the IABP and NCEP-NCAR data. The magnitude of wind speed can not be compared directly because of different natures of the wind products (IOEB measured wind at about 2 m height while IABP provides geostrophic wind and NCEP-NCAR gives 10 m wind). The magnitude of SLP also varies among three data sets. The temporal variations of winds and SLP, however, are quite consistent.

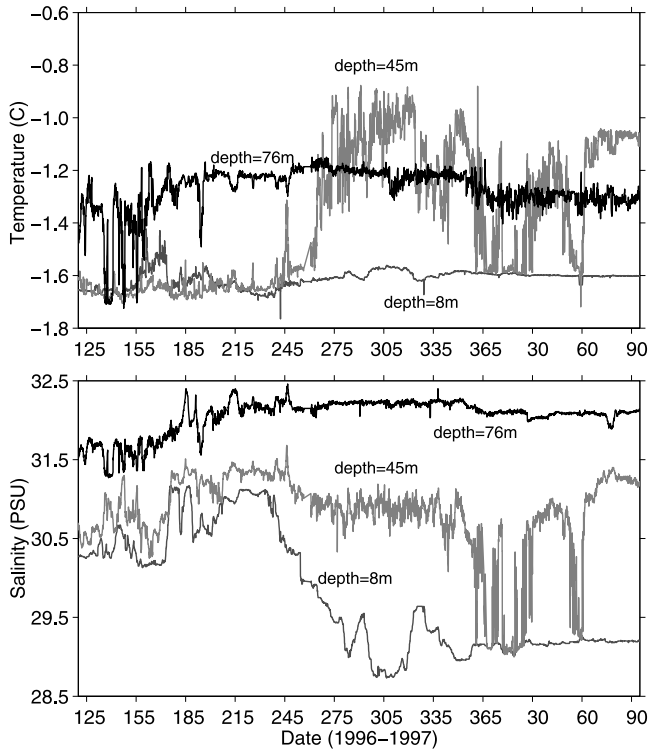

Figure 4. Temperature and salinity between the first refurbishment in April 1996 and the second in April 1997.

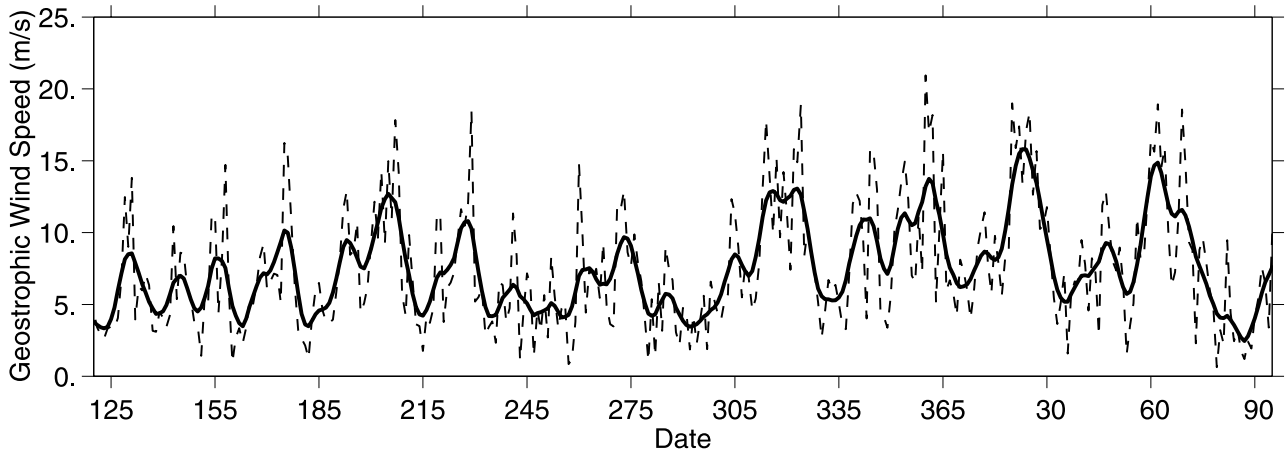

Figure 5. Geostrophic wind speed (from the International Arctic Buoy Program) at the buoy site for the period between refurbishments (dashed line is for the daily wind speed and the solid line is for its 5-day running mean). (Unit: m s^{-1}.)

The agreement between IOEB and IAPB appears to be better than that between IOEB and NCEP-NCAR.

3. Mixing Events Observed by IOEBs

[9] From the IOEB observations of salinity and temperature, we have identified a few mixing events that reached the halocline depth, characterized by either complete or partial homogenization of water properties in the mixed and halocline layers. In this section we describe and explain them in the context of SLP and geostrophic wind variations.

3.1. Beaufort Sea Buoy

[10] The first IOEB was deployed in the Beaufort Sea from an ice camp at 73°N, 148°W in April 1992 (Figure 2). Because of failure of the CT recorders, hydrographic data were not collected during this deployment (see *Krishfield et al.* [1999] for an explanation). The buoy was recovered and refurbished in April 1996, so that afterward both temperature and salinity were measured at three depths (8, 45, and 76 m). These depths were chosen to cover the Arctic Ocean mixed layer, the halocline and the upper thermocline. The satellite-transmitted data were recorded at a temporal resolution of 6 hours (the data recovered with the instrument had a higher frequency of 1 hour). The buoy, which was refurbished roughly a year later in April 1997, continued to drift anticyclonically following the Beaufort Gyre until it ran aground in a shallow shelf area in early 1998. While the meteorological, ice and other oceanographic data (such as current velocity from the

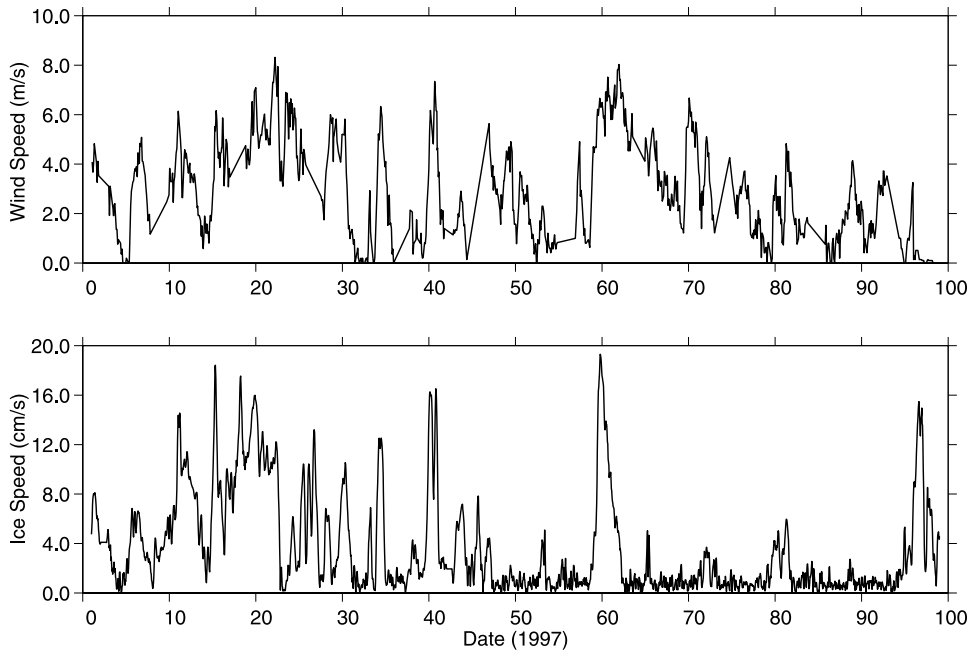

Figure 6. Speeds of surface wind and ice drift measured by the buoy (unit: m s^{-1} for wind and cm s^{-1} for ice).

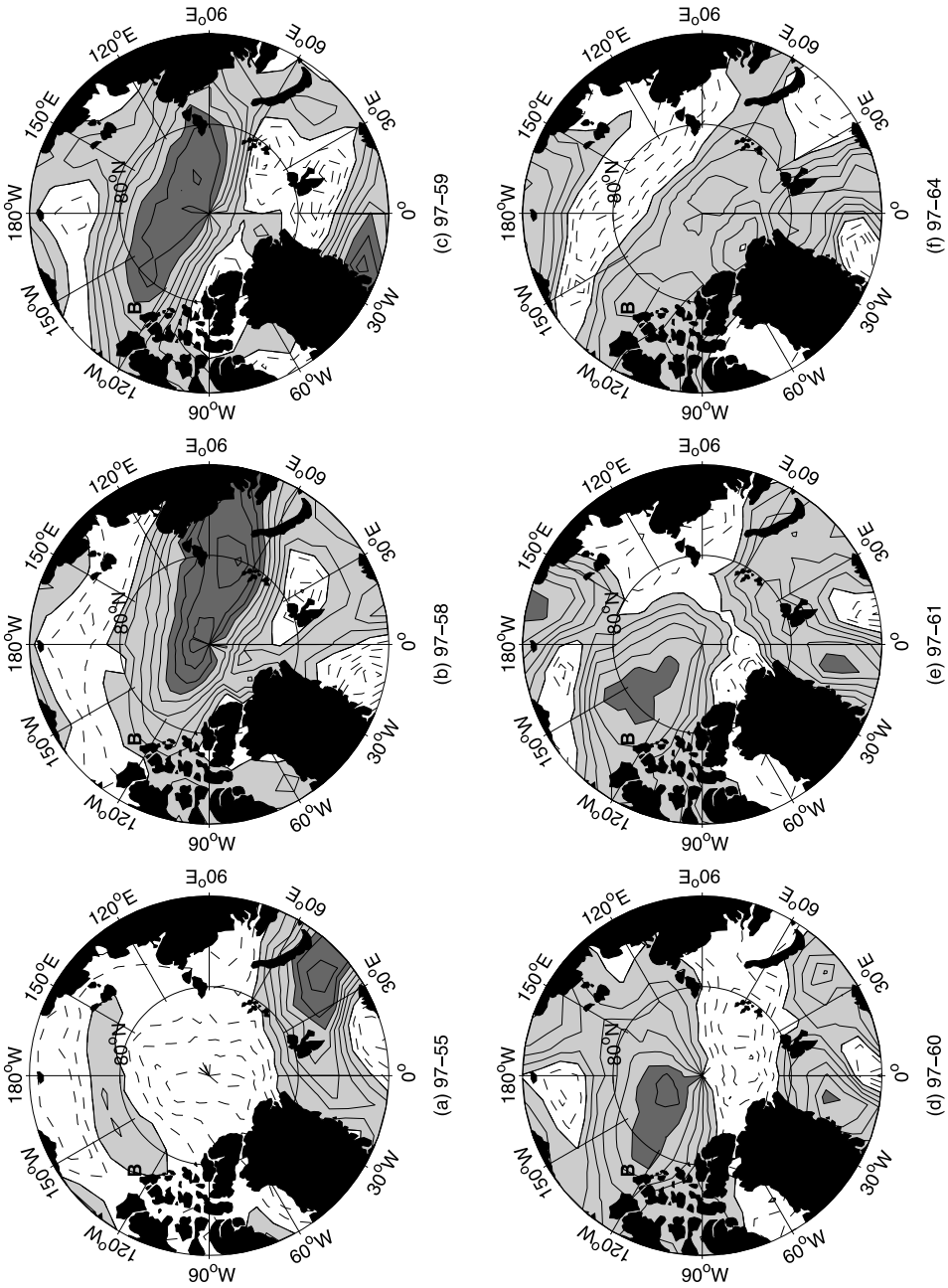

Figure 7. Anomalous geostrophic wind speed between the 54th and 65th day in 1997 (m s^{-1}). The contour interval is 2 m s^{-1}, with solid and dashed lines for positive and negative anomalies, respectively. Areas of positive anomalies are also shaded. The darker shaded areas are for anomalies that exceeded 10 m s^{-1}. The location of the buoy is marked by **B**, which was just west of 120°W.

ADCP) collected before the April 1996 refurbishment are still very useful for studying some important dynamical processes (such as internal waves), we focus on data from the period when hydrography was observed, from April 1996 to the end of 1997.

[11] Between the first and second refurbishing (April 1996 and April 1997), the IOEB drifted mainly southward just offshore of the 3000 m isobath (Figure 3). The salinity and temperature observed during this period are shown in Figure 4. The buoy seems to pass from one hydrographic regime to another around the 240th day (27 August) in 1996. Before that the water temperature at 45 m was near the freezing point, similar to that at 8 m. The salinity at 8 m was also considerably higher, between 30 and 31 psu. It appears that both temperature and salinity at 8 and 45 m were quite homogenized. This suggests that the mixed layer during this period was abnormally deep compared to a typical Arctic mixed layer of 20–30 m. After the 240th day the water mass at 8 and 45 m gradually show distinctly different characteristics. The temperature at 45 m rises gradually to about $-0.8°$ and surface salinity at 8 m decreases to about 29 psu. The vertical structure became

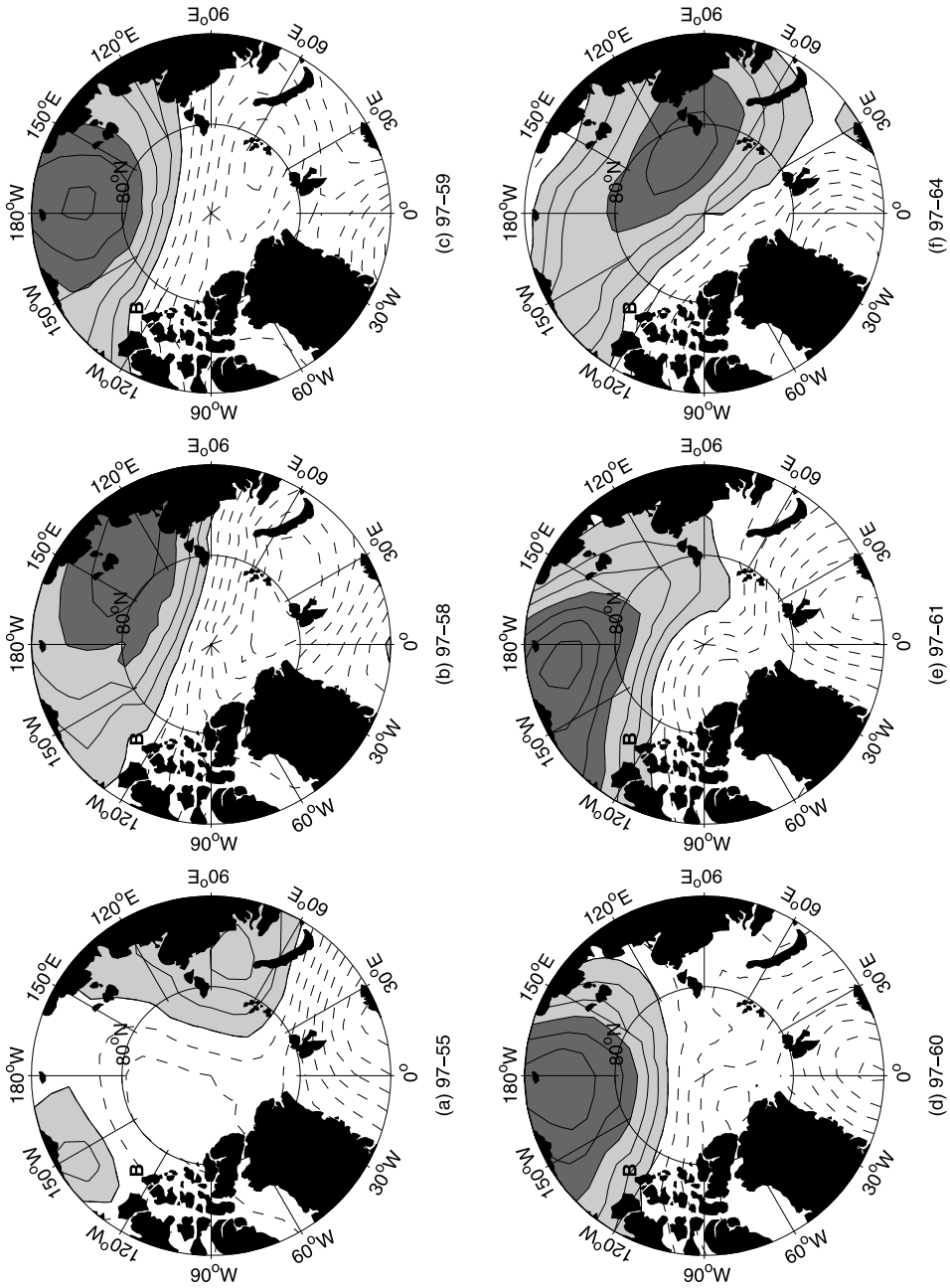

Figure 8. Anomalous SLP between the 55th and 64th day in 1997. The contour interval is 4 mb, with solid and dashed lines for positive and negative anomalies, respectively. Areas of positive anomalies are also shaded.

more 'typical' of the western Arctic Ocean, with a fresh, cold mixed layer overlying warmer, saltier water, with water properties strongly influenced by water from Bering Strait. It is interesting to note that the buoy was nearly stationary just north of 79°N before the 240th day, but drifted much more rapidly toward the south afterward. Thus the observed changes in temperature and salinity may be primarily due to the change of water mass properties along the buoy trajectory.

[12] Near the end of 1996 and into early 1997 there appear to have been some mixing events that reached the halocline layer. Either because of rapid restratification or because of quick passage through the mixing area, the typical mixed layer and halocline structure is observed again within only a few days. Another mixing event occurred on around the 60th day in 1997. The salinity at 8 m, about 29 psu, was about 1 psu lower than that at 45 m, and remained low through the mixing events. Thus it is unlikely that the mixing was driven by brine rejection. It is more likely that these events were mechanically forced by storms, as has been reported by *Steele and Morison* [1993] and *Yang et al.* [2001]. Therefore we will examine surface atmospheric conditions in the vicinity of the buoy during the observed mixing events.

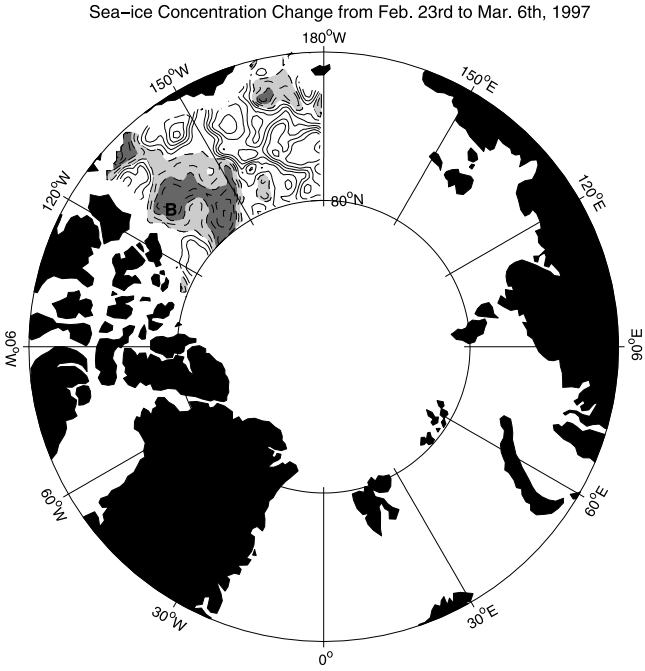

Figure 9. The change in sea ice concentration between the 54th (23 February) and 65th day (6 March) in 1997 (satellite SSM/I data). The contour interval is 2%, with solid and dashed lines for positive and negative anomalies, respectively. The negative areas of sea ice anomaly are shaded.

[13] We have analyzed two different sets of meteorological data, the surface wind measured by IOEBs, and the geostrophic wind and SLP from the IABP. In addition, we have used the surface wind and SLP from the NCEP-NCAR reanalyses for comparison and for examination of long-term variability. Surface wind data taken directly from IOEBs would be ideal for this study since they were collected simultaneously with ice and oceanic observations at precisely the same location. However, as discussed by *Krishfield et al.* [1999], the wind sensor could have occasionally been partially or completely frozen by ice, sometimes resulting in an underestimate of surface wind speed. Therefore, in addition to wind data from the IOEBs, we will also use the meteorological data from the IABP.

[14] The geostrophic wind speed at the buoy site is shown in Figure 5 (the dashed line is for the daily speed and the solid line is for its 5-day running mean). We have compared this with the surface wind speed measured directly by the buoy. Their temporal variations agree well (the amplitude of the surface wind was understandably smaller than that of geostrophic wind) except for a period near the end of 1996 when the IOEB wind speed was near zero. We believe that this was due to the instrument's rotor being frozen. Both types of data show that the wind speed was considerably higher near the end of 1996, in early 1997, and around the 60th day in 1997, coinciding with the three periods in which deep mixed layers were observed. Although the wind speed was high on around day 320 in 1996, the hydrographic data, however, did not show a complete homogenization between 8 and 45 m. The density difference between these two levels did decrease in this short period, as the surface salinity increased and the subsurface temperature at 45 m increased. Whether this was due to a partial mixing, or whether the buoy was just passing through a previously mixed area is not clear at this point.

[15] The development of each of three storms (near the end of 1996, early in 1997, and on day 60 in 1997) was quite similar in terms of SLP anomaly evolution. Thus here we will only discuss the storm on the 60th day in 1997, since it was more distinct in time from other storms. Near day 60 the speed of both ice motion and surface wind increased considerably (Figure 6). The ice was moving at about 1–3 cm s^{-1} before the storm and accelerated to nearly 20 cm s^{-1}. The wind speed at the buoy height (2 m) also increased to about 8 m s^{-1}. Geostrophic wind anomalies and SLP at 12:00 hours from the 55th to the 664h day in 1997 are shown in Figure 7. The anomalous data were based on the twice daily climatology calculated between 1 January 1979 and 31 December 2000 using IABP data. The buoy site is marked by a "**B**". The wind speed near the buoy increased on the 55th day, growing gradually to a maximum (about 10 m s^{-1} higher than climatology) on the 59th day. The positive anomaly of wind speed lasted for more than 10 days, and was still present on the 64th day. A notable feature in Figure 7 is that the buoy was seldom in the center of the area of maximum wind speed, but was rather on the edges of this area. The maximum wind speed anomaly was near 20 m s^{-1}.

[16] The SLP anomaly exhibited a dipolar structure (Figure 8). A pair of high- and low-SLP centers appeared on the 55th day, with a positive SLP anomaly in the Kara Sea (centered at about 65°E, 75°N), and a negative center in the Greenland and Norwegian Seas just south of Fram Strait (at about 15°E, 70°N). This dipole intensified and

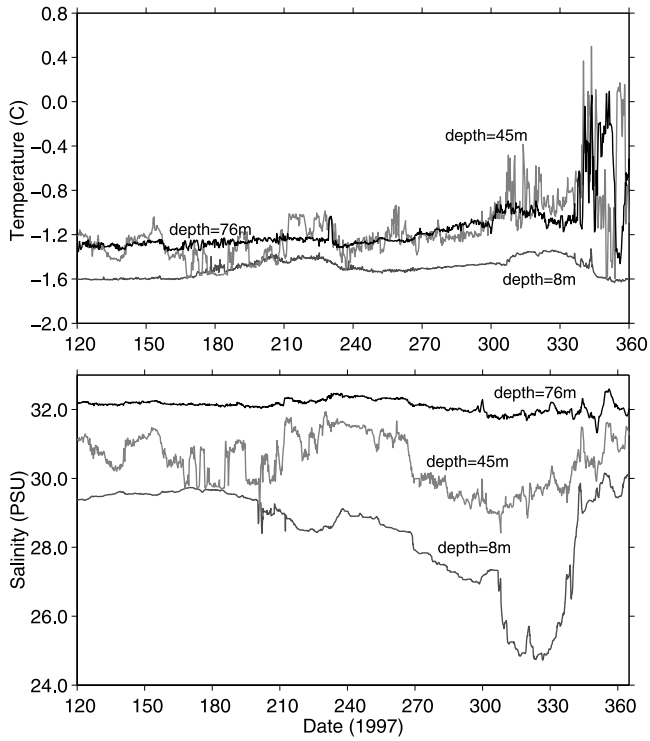

Figure 10. Temperature and salinity after the second refurbishment in April 1997.

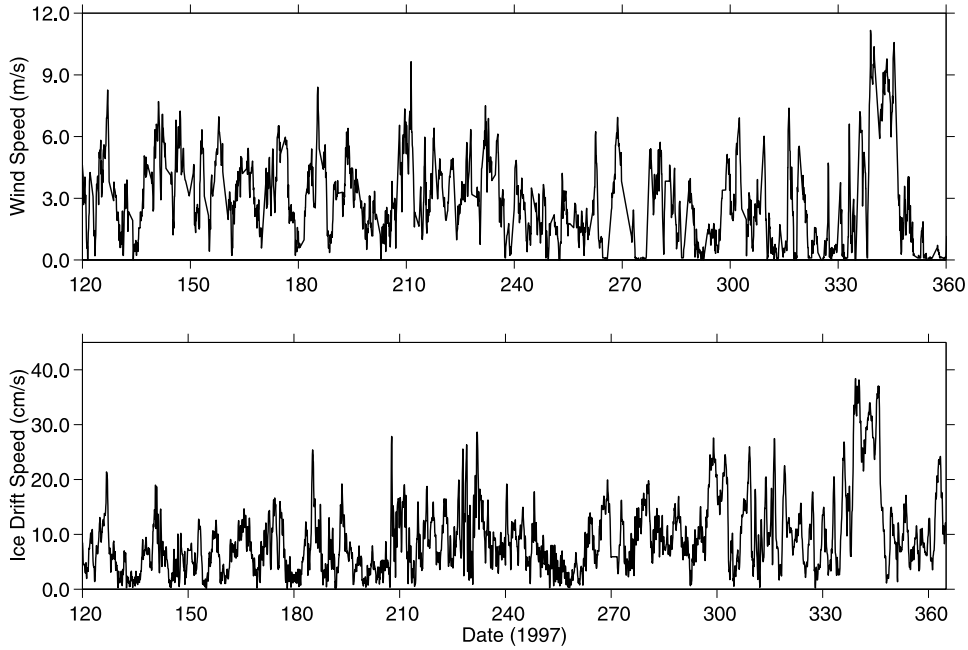

Figure 11. Speeds of surface wind and ice drift measured by the buoy (unit: m s^{-1} for wind and cm s^{-1} for ice).

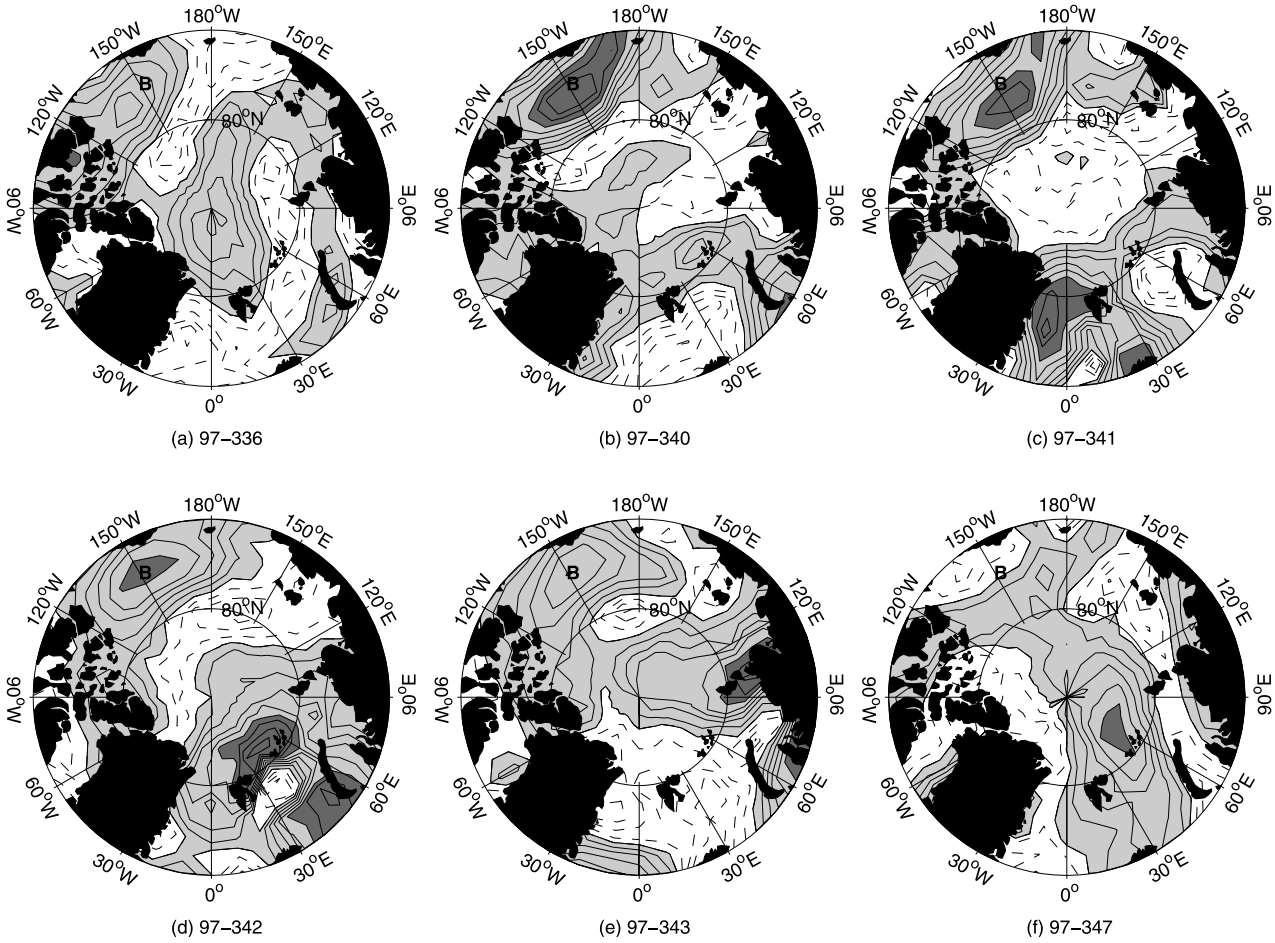

Figure 12. Anomalous geostrophic wind speed between the 336th and 347th day in 1997 (m s^{-1}). The contour interval is 2 m s^{-1}, with solid and dashed lines for positive and negative anomalies, respectively. Areas of positive anomalies are also shaded. The darker shaded areas are for anomalies that exceeded 10 m s^{-1}. The location of the buoy is marked by **B**, which was just west of 150°W.

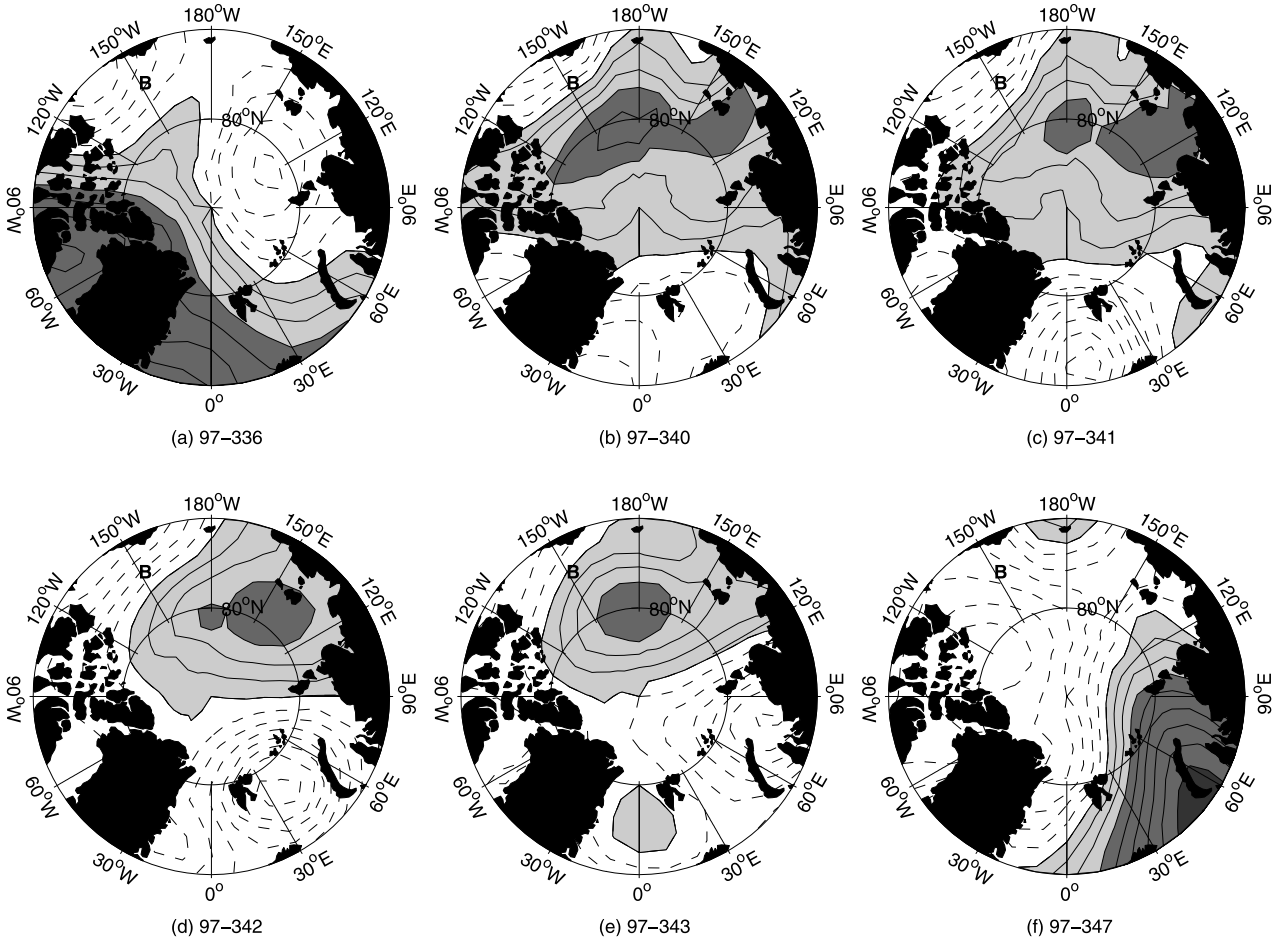

Figure 13. Anomalous SLP between the 336th and 347th days in 1997. The contour interval is 4 mb, with solid and dashed lines for positive and negative anomalies respectively. Areas of positive anomalies are also shaded.

propagated eastward slowly in the first several days. The low then moved poleward after the 58th day, while the high continued eastward toward the East Siberian and Chukchi Seas. Later, the low-pressure center started to diminish near the North Pole, but another low started developing south of Fram Strait. The new low-SLP center appeared to split into two parts which propagated in opposite directions. The pressure gradient was large between the high- and low-SLP centers and hence the geostrophic wind was strong in those areas (Figures 7 and 8). The buoy was located in one of those areas.

[17] How did the sea ice concentration respond to this synoptic-scale atmospheric forcing? To answer this question, we examined the daily ice concentration data from satellite passive microwave sensors. The data, derived using the bootstrap method as described by *Comiso* [1995], were obtained through the National Snow and Ice Center. It is obvious that the concentration is one index for the total sea ice change, but is also a very useful indicator of divergence and convergence of ice drift, especially on synoptic timescales over which the change in thickness due to melting and freezing is probably small. The sea ice concentration near the buoy was higher than 90% (not shown) before the storm developed, typical of winter sea ice conditions in this area. The change of ice concentration between the 54th day (23 February) and the 65th day (6 March) is shown in Figure 9. The ice concentration at the buoy site had decreased by about 7 to 8% after the storm. The ice concentration became lower in the Beaufort Sea (between 120°W and 150°W) and higher in the Chukchi Sea (between 150° and 180°W). This was mainly due to changes in sea ice transport driven by the wind stress. During the storm development, the Beaufort Sea and Chukchi/E. Siberian Seas were dominated by low- and high-pressure centers, respectively. Thus the anomalous geostrophic wind at the buoy site was mainly southward. This drove the sea ice transport toward the high-SLP center because of the Coriolis effect. This is confirmed by the speed of the drifting buoy (which was fixed in the pack ice). Just before the storm on day 54 the buoy drifted at a speed of about 0.2 cm s^{-1} toward the west and about 0.004 cm s^{-1} toward the south. At the peak of the storm development on the 60th day, the southward velocity increased to 13 cm s^{-1} and the westward velocity to 4 cm s^{-1}, consistent with our assessment of ice convergence and divergence.

[18] The development of the other two storms, one near the end of 1996 and one in January 1997, also involved both high- and low-SLP centers. For example, the geo-

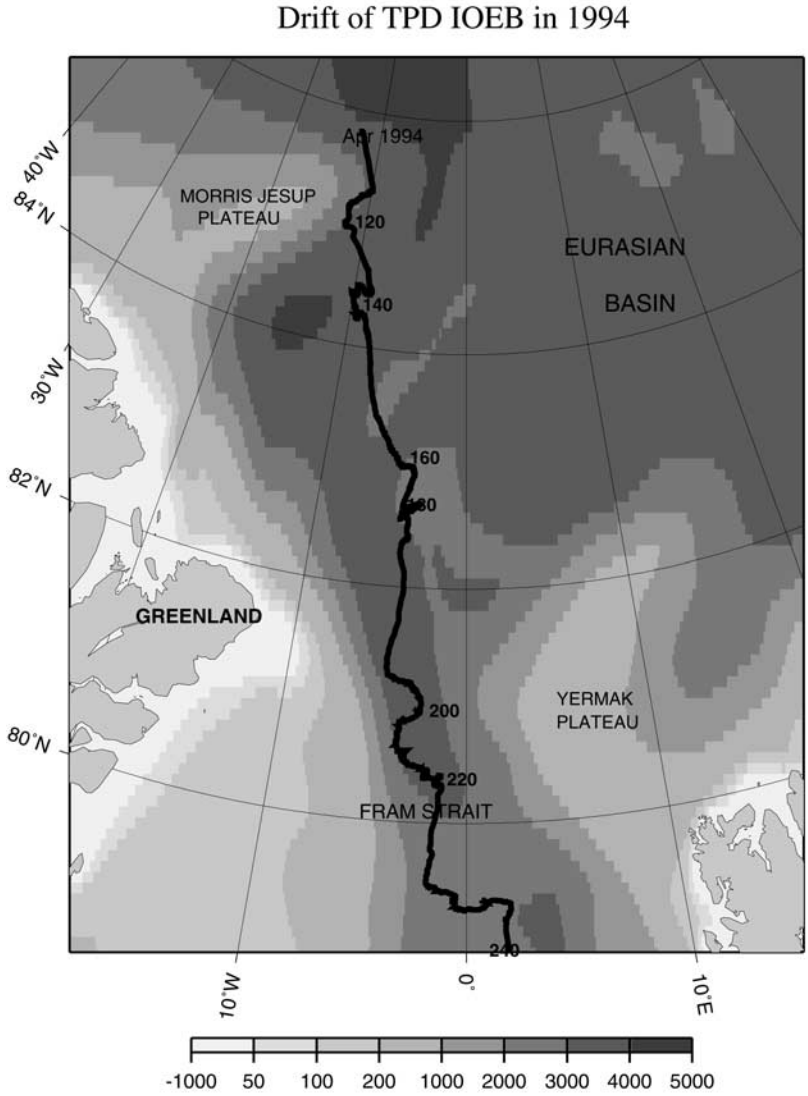

Figure 14. The trajectory of the transpolar IOEB.

strophic wind was more than 15 m s^{-1} higher than its climatology on the 19th and 20th day in 1997. The SLP anomaly was almost a mirror image of that on the 60th day, with high SLP over the Chukchi and East Siberian Seas and low SLP in the Beaufort Sea and the Canadian Archipelago. The change in sea ice concentration after this storm was very similar to what was just discussed in connection with Figure 9.

[19] The IOEB was refurbished again in April 1997 and continued to drift anticyclonically in the Beaufort Gyre (Figure 2). The hydrographic data collected after this refurbishment are discussed by *Yang et al.* [2001], who suggest that the rapid change of salinity and temperature in December 1997 (Figure 10) was due to storm-forced mixing. This hypothesis is consistent with the estimate of turbulent kinetic energy flux calculated from buoy-observed wind and ice drift speeds (Figure 11). Here we examine in more detail the development of the storm and study its impact on sea ice distribution. Figure 12 shows that the geostrophic wind speed in this period was relatively strong in the western Arctic where the buoy was located (the buoy location was marked by **B** in Figures 12 and 13). The buoy was near the center of maximum wind on the 340th day (Figure 12b), with wind speeds more than 20 m s^{-1} stronger than climatology. The buoy stayed in the center of the wind speed maximum for another 5 days until the 345th day (although the wind speed weakened gradually). This strong wind condition was caused by an anomalously high-SLP center over the Laptev and northern Chukchi Seas just south of the North Pole, and a low-SLP condition in the southern Beaufort and Chukchi Seas. The pressure gradient associated with these SLP centers created a strong westward wind in the Beaufort Sea area where the IOEB was located. As Figure 13 shows, this pressure anomaly persisted at the same location for several days, from the 339th to the 345th day. This was consistent with the buoy-observed surface wind conditions in this period [*Yang et al.*, 2001]. Because of the strong eastward winds, sea ice concentration after the storm increased considerably in the southern Chukchi Sea and decreased in a broad area within the Beaufort Sea. The ice concentration at the buoy site changed from near 100% on day 335 to about 92% on day 346. It should be noted that

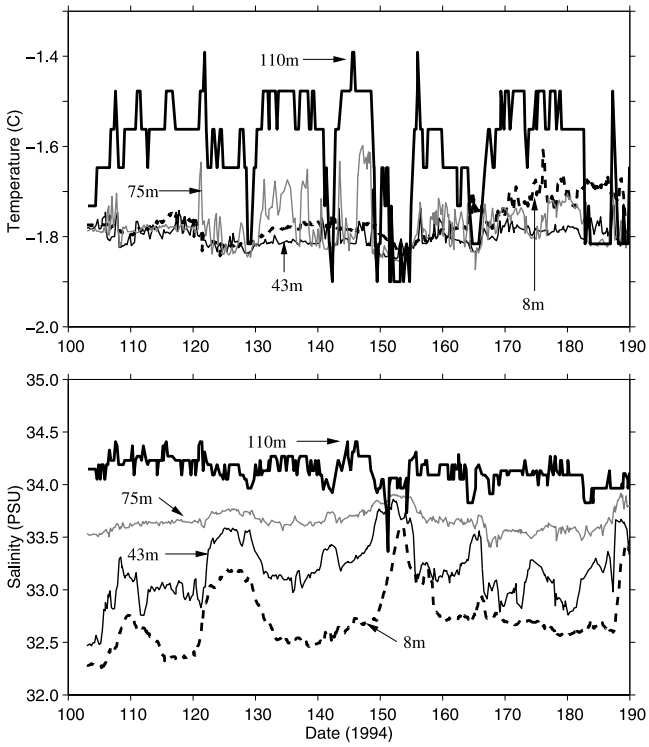

Figure 15. The temperature and salinity measured by the transpolar buoy.

this reduction occurred during the season of maximum ice growth.

[20] The IOEB continued to drift after the end of 1997 (see trajectory in Figure 3), eventually entering the shallow shelf area of the Chukchi Sea. Oceanographic conditions over the shelf are considerably different from these in deeper waters. Water mass characteristics on the shelf are more influenced by coastal processes such as tidal mixing, coastal upwelling, shelf-basin interactions, etc. These are interesting topics, but clearly beyond the scope of this study.

3.2. Transpolar Drift Buoy

[21] In the preceding section we discussed some cases of mixing events and their association with synoptic storms in the Beaufort Sea. Water mass characteristics in the upper Beaufort Sea are strongly influenced by Bering Seawater, and so are considerably different from those in the Eurasian Basin, where Atlantic inflow plays a greater role. Fortunately, an IOEB was deployed in April 1994 in the Transpolar Drift ice stream at 86°N, 12°W (see Figure 2 for the buoy location). It eventually drifted through Fram Strait and was recovered after 9 months at 9°W, 74°N in the Greenland Sea (see Figure 14 for the buoy trajectory). About day 190 (9 July) the buoy passed through Fram Strait and into the Greenland Sea. *Yang et al.* [2001] have discussed briefly the hydrographic changes observed by this IOEB, for the purpose of showing that deep vertical mixing was not restricted to the Beaufort Sea. Here we examine storm development during each of the IOEB-observed mixing events, and the associated sea ice response. Like *Yang et al.* [2001], we use only those data collected north of Fram Strait (before the 190th day) since oceanographic conditions in the Nordic Seas are very different from those in the Arctic Ocean.

[22] For the Transpolar Drift IOEB, temperature and salinity observations were made at 4 depth levels: 8, 43, 75, and 110 m. Like the Beaufort Gyre IOEB, the top two levels nicely capture variations in the mixed layer and halocline. The thermocline is deeper north of Fram Strait than in the Beaufort Sea, so the additional sensors at 110 m were ideal for our study. Temperature and salinity along the

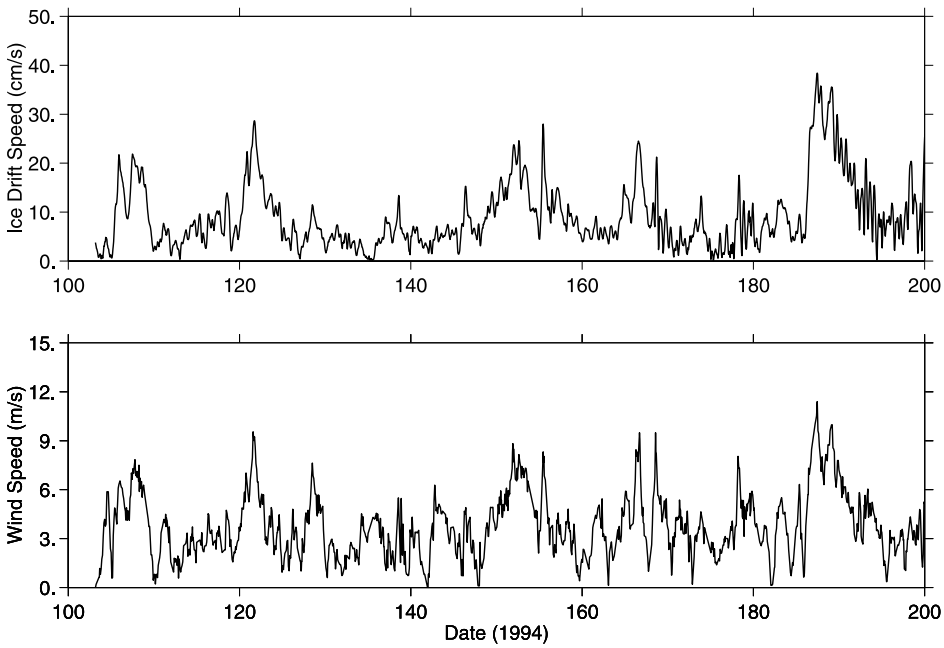

Figure 16. The speeds of surface wind and ice drift measured by the buoy (unit: m s^{-1} for wind and cm s^{-1} for ice).

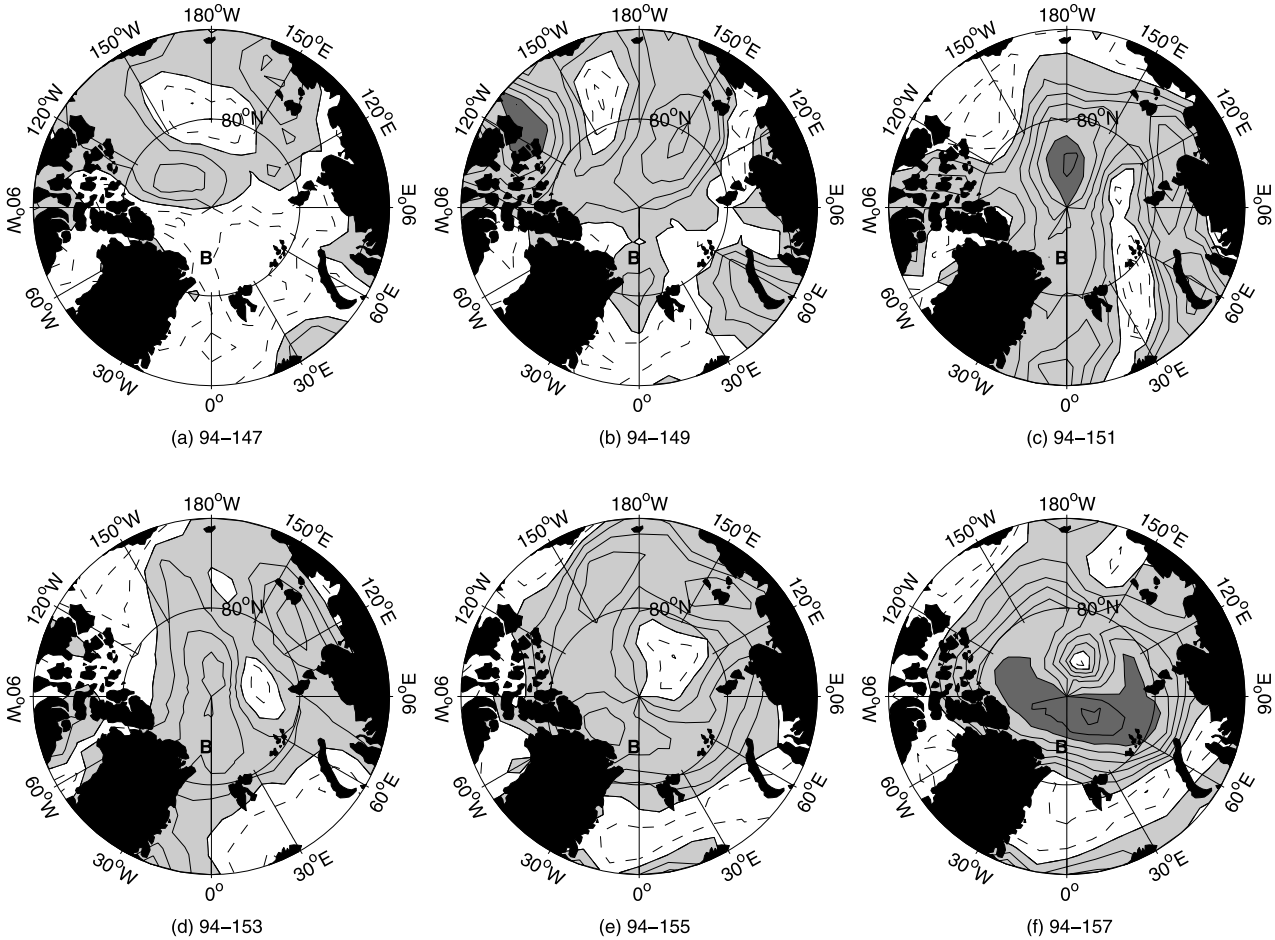

Figure 17. Geostrophic wind anomalies between the 146th and 157th day in 1994 (m s^{-1}). The contour interval is 2 m s^{-1}, with solid and dashed lines for positive and negative anomalies, respectively. Areas of positive anomalies are also shaded. The darker shaded areas are for anomalies that exceeded 10 m s^{-1}. The location of the buoy is marked by **B**, which was just north of Fram Strait.

buoy trajectory are shown in Figure 15, and the speeds of surface wind and ice drift are presented in Figure 16. On five separate occasions the temperature at all four depths appears to be homogeneous: on the 129th day, the 142nd, between the 149th and 154th days, on the 165th day, and between the 185th and 190th days (Figure 15a). Interestingly, salinities were not completely homogenized over this depth range. A possible explanation is that in the Arctic Ocean mixing with subsurface warm water is often followed by melting of sea ice, which cools the mixed layer rapidly toward the freezing point, and also results in an immediate restratification of the mixed layer due to the meltwater. This has been discussed in many previous papers [e.g., *Moore and Wallace*, 1988]. In the third and fifth cases mentioned above, the salinity did show some sign of mixing (i.e., increase of surface salinity and decrease of subsurface salinity). So we will focus on these two cases, for which we have greater confidence that deep mixing actually occurred.

[23] Let us first examine the event occurring around the 150th day in 1994. During this period the geostrophic wind was stronger over most of the Arctic basin, especially near the North Pole in the area north of 80°N (Figure 17). Near the buoy site (marked by "**B**") the wind speed started to increase on the 148th day, reaching a maximum around the 157th day, when the wind speed was almost 10 m s^{-1} higher than normal. It also appears that the center of the positive wind anomaly moved slowly eastward (cyclonically). The SLP was lower almost everywhere over the Arctic basin (Figure 18). A low-SLP center initially emerged from the Nordic Sea area and moved toward the Barents Sea on the 148th and 149th days. This intensified quickly, while moving slowly northeastward. The cyclonic wind anomaly induced by this low-SLP center was mainly responsible for the change in wind speed seen in Figure 16. Sea ice concentration in the vicinity of the buoy was changed only 2 to 4% by the storm (Figure 19). The presence of a low-SLP center in the Eurasian basin increased the zonal SLP gradient, and thus southward transport of sea ice associated with the Transpolar Drift should increase north of Fram Strait. However, this also occurred in the marginal ice zone during the melting season, so the net change in ice concentration may not have been dominated by storm forcing. The sea ice concentration did increase noticeably in the western Arctic and north of Fram Strait, and

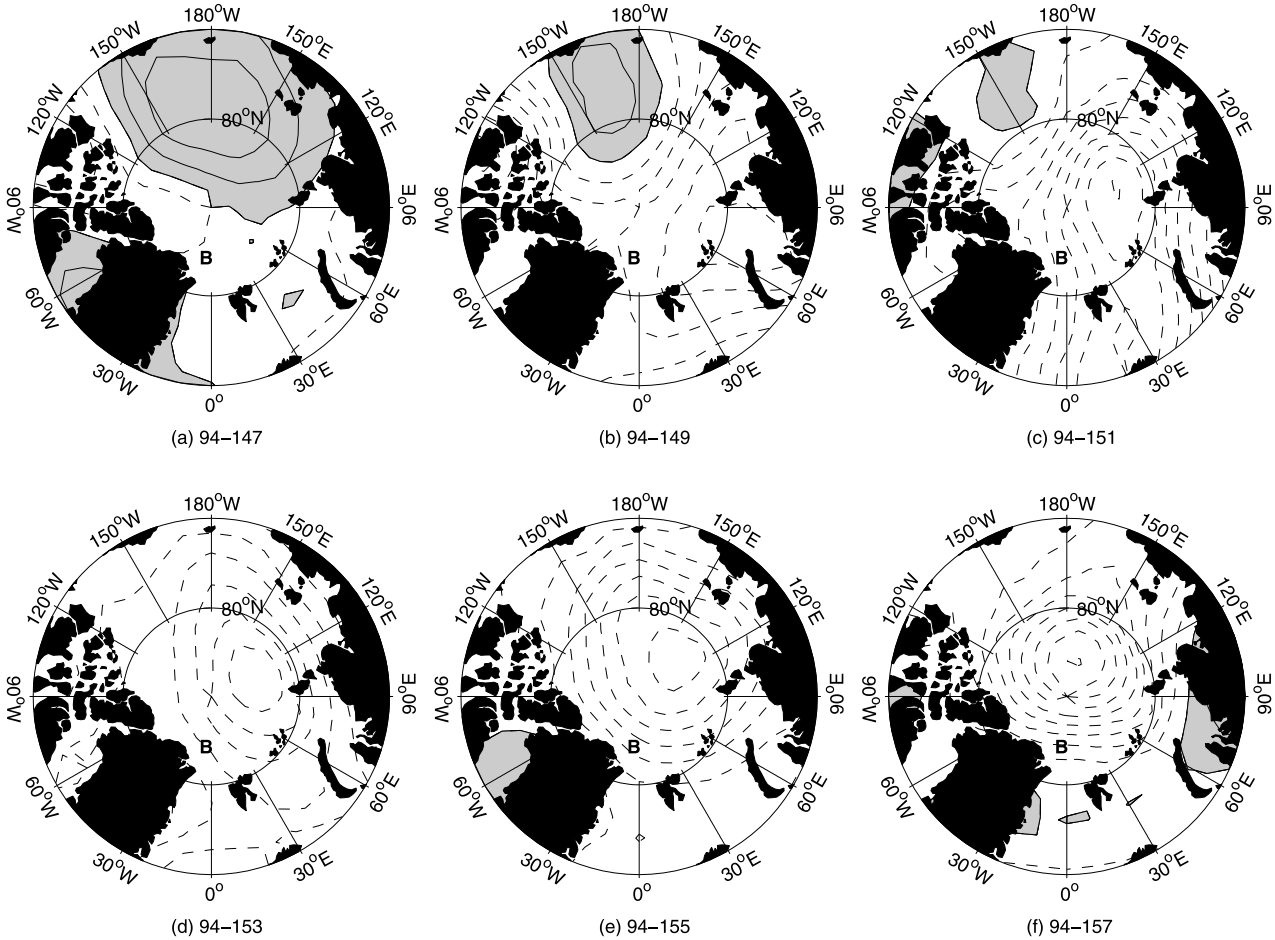

Figure 18. The anomalous SLP between the 146th and the 157th day in 1994 (mb). The contour interval is 4 mb, with solid and dashed lines for positive and negative anomalies, respectively. Areas of positive anomalies are also shaded.

decreased in the Eurasian basin, consistent with what would be expected from a wind field associated with a low-SLP center in the Eurasian basin.

[24] Another strong wind condition developed just before the IOEB passed through Fram Strait. Like the previous event, there was only a mild increase in wind speed (about $7-8$ m s^{-1}), which lasted about one week near the IOEB location. The SLP field, however, was quite different from the previous cases. This case involved a dipole of low- and high-SLP centers. The high was initially located in the Laptev Sea area and then moved toward the North Pole, and a low then developed in the area around Fram Strait. The pressure gradient led to strong winds at the buoy location, causing upper ocean mixing.

[25] We have discussed four mixing events observed by IOEBs, two in the Beaufort Sea and two in the Transpolar Drift area just north of Fram Strait. Daily geostrophic winds from the International Arctic Buoy Program show that wind speeds were abnormally high when mixing was observed, consistent with the buoy surface wind data. SLP patterns which led to ''gusty'' winds were not unique. In the Beaufort Sea the SLP showed a dipolar structure during both mixing events. North of Fram Strait the SLP anomaly was different for each of the three mixing events: it involved a low-SLP center in the first case, a high in the second, and a dipolar structure in the third case.

4. Basin-Wide Occurrences of Mixing and Temporal Variations

[26] Whenever the mixed layer deepens, warmer subsurface water is drawn toward the surface layer, and a warmer mixed layer will affect ice-water heat fluxes, and thus the sea ice distribution. The importance of storm-driven mixing to the heat and salt budgets of the upper Arctic Ocean depends on how stormy the Arctic is. Mixing events occurred several times within the short period of IOEB observation, suggesting that storm forcing may be an important contributor to upper ocean mixing. It should be pointed out that most mixing events identified by IOEB data were rather shallow, and reached only the halocline or the upper thermocline. On the other hand, the IOEBs were usually not in the area of maximum wind speed when the events occurred. It is reasonable to assume that mixing could reach deeper levels in areas with stronger winds, and could consequently entrain more warm water from below into the mixed layer.

[27] In situ measurements of storm-driven mixing events are rare. Numerical modeling will be useful to quantify the

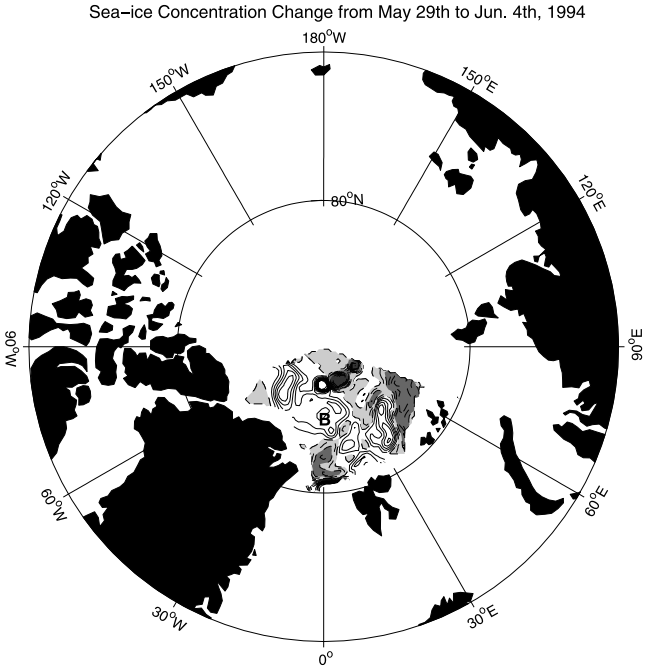

Figure 19. The change in sea ice concentration between the 149th (29 May) and 156th (4 June) day in 1994 (satellite SSM/I data). The contour interval is 2%, and areas of negative sea ice anomaly are shaded.

heat and salt fluxes associated with vertical mixing. This is beyond the scope of this paper. Here we will only examine the wind field and its variability. We will first examine the climatology of the wind field before discussing its interannual variations. The IABP data were used to compute a 22-year climatology of daily geostrophic wind. The monthly averaged wind speeds for February, May, August, and November are shown in Figure 20, representing the four seasons. In general, the climatological wind speed is weaker than 10 m s^{-1} in almost the whole Arctic basin. It is considerably stronger in fall and winter than in summer and spring, consistent with the seasonal variations described by *Polyakov et al.* [1999]. Wind speed is greater in areas north of the Atlantic and Pacific inflows, such as in the Nordic Seas, the Barents Sea, and the Chukchi Sea, but weaker in areas off the Canadian and Eurasian coasts. Next, we will compute the number of stormy days, defined here as the number of days when the daily averaged wind speed was greater than 15 m s^{-1}. In the Arctic, storms can be either cyclonic or anticyclonic. We will not attempt to separate them in this study, since we are interested primarily in the wind speed. The seasonal distribution of synoptic activity, including both cyclones and anticyclones, has been discussed nicely by *Serreze and Barry* [1988].

[28] The 22-year averaged number of stormy days, between 1979 and 2000, is shown in Figure 21. In the vast area of the Arctic Basin the average number of days with such strong wind was less than 25, except in the area north of Fram Strait and in the Nordic Seas. Using a lower threshold of 15 m s^{-1} gives a similar spatial pattern, although values change somewhat. To investigate interannual variations, we have computed the ''anomalous'' number of ''stormy days,'' shown in Figure 22. The number of stormy days was generally lower in the 1980s than in the 1990s. Between 1980 and 1984, the whole Arctic was relatively calm (Figure 22a). This condition persisted in most of the Arctic in the period between 1985 and 1989 except in the eastern basin between 90°E and 150°E (Figure 22b). The 1990s were much stormier in the whole Arctic (Figures 22c–22d). It has been reported that the halocline in the Eurasian Basin has been retreating in the past decade [*Steele and Boyd*, 1998]. One hypothesis advanced to explain the vanishing halocline was an increase in Atlantic inflow through Fram Strait and the Barents Sea. Here we have shown that the weather in this region became stormier in the 1990s. Thus one may speculate that enhanced storm-driven mixing may have played a role in bringing warmer Atlantic water to the surface, and perhaps contributed to the retreat of the Arctic halocline.

[29] It should be noted that in the Central Arctic, the year with the most storm is 1997 while the year with the second most storm is 1996 which are the same years when the IOEB was providing good data. Although the IOEB provides very good temporal resolution, it is not able to provide good spatial details about storm occurrences. The deployment of more of these buoys at other areas of the basin is thus most desirable for a more detail study of the mixing phenomenon.

[30] Does the Arctic Oscillation affect storm distribution? We have computed the correlation between the annual AO index [*Thompson and Wallace*, 1999] and the number of stormy days in a year (as in Figure 22) for the period from 1979 to 2000. The correlation is rather lower, between −0.6 and +0.4 for this short period. The correlation is positive, although low, in most of the Arctic basin except in the western Beaufort Sea, Chukchi Sea, East Siberian Sea, and southern Laptev Sea (Figure 23). The correlation is not significant statistically in almost the whole basin. We have also used longer records from NCAR-NCEP (1947–2000) and find a similar pattern.

[31] The flux of kinetic energy is just one factor; mixing also depends on local buoyancy fluxes and background stratification. In winter, brine rejection weakens the stratification, which, together with strong wind forcing, may make deep mixing events more likely. Another factor is sea ice concentration and its response to wind forcing. Previous studies have shown that ice drift speeds respond rather rapidly to wind forcing [e.g., *Colony and Thorndike*, 1984]. This was confirmed by the IOEB measurements of ice and wind speed. During storms both wind and ice speeds increased almost simultaneously. We are mindful, however, that using wind speed alone could oversimplify the problem.

[32] It is shown that storm-driven mixing can contribute to the fluxes of heat and salt to the surface mixed layer. To assess the contribution of this process to the overall heat budget of the Arctic Ocean mixed layer requires good quality data of surface fluxes of buoyancy and momentum, and models that can simulate well the mixing process. This is clearly beyond the scope of this study. Unlike the solar radiation which warms up the mixed layer gradually in the summer season, storm mixing is highly nonlinear and can change the mixed layer temperature and salinity

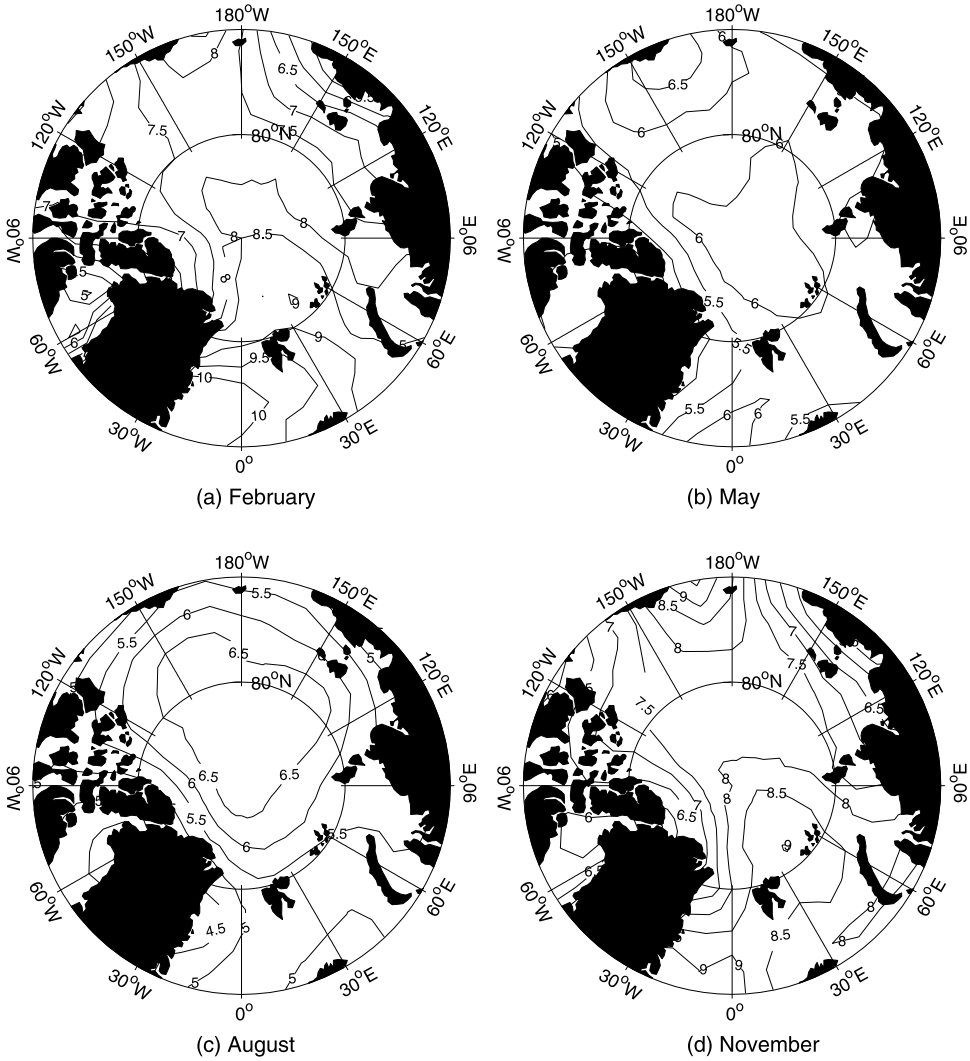

Figure 20. Geostrophic wind speed for February, May, August, and November (unit: m s^{-1}). The data are based on the 22-year climatology averaged between 1979 and 2000.

dramatically within days. This was clearly shown in the Beaufort Sea in late 1997. The mixed layer salinity increased more than 4 psu just within a few days. The heat flux was also significant and resulted in noticeable melting of sea ice in storm area [*Yang et al.*, 2001]. More important, the stratification of the upper Arctic Ocean was weakened significantly. This made the Arctic Ocean more vulnerable for deep mixing. We speculate that storm-driven mixing does play an important role in the Arctic Ocean mixed layer heat and salt balances.

5. Discussion and Summary

[33] We have investigated IOEB observations of oceanic, atmospheric, and ice parameters from April 1996 to the end of 1997 in the Beaufort Sea, and from April through July 1994 in the area north of Fram Strait. The buoy data show water mass characteristics typical of the Arctic Ocean (i.e., a cold halocline layer "sandwiched" between a cold, fresh mixed layer and a warmer, saltier thermocline layer below). The vertical gradient of salinity is large because of the presence of the halocline layer, as pointed out in many

Figure 21. The average number of "stormy" days (with daily average geostrophic wind speeds greater than 15 m s^{-1}) per year between 1979 and 2000. The contour interval is 2 days.

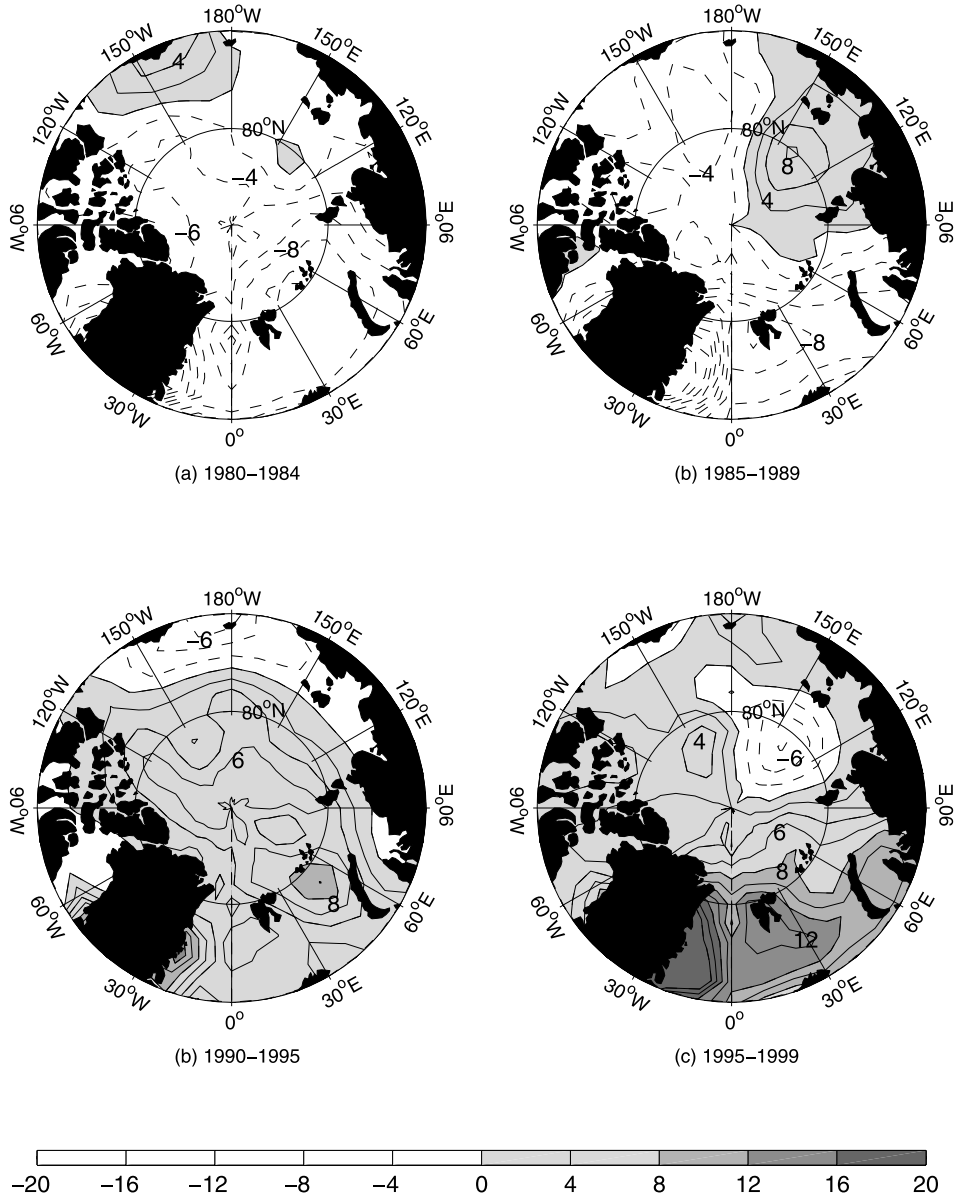

Figure 22. The anomalous number of stormy days per year averaged for a 5-year period: (a) 1980–1984, (b) 1985–1989, (c) 1990–1994, and (d) 1995–1999. The contour interval is 2 days. Areas of positive anomaly are shaded.

previous studies. The prevailing view in the Arctic Ocean research community is that strong stratification should prevent vertical mixing from penetrating the Arctic halocline, and thus halocline water is likely to originate in remote areas such as coastal polynyas, where brine rejection is greater [e.g., *Aagaard et al.*, 1981]. This view has been supported both by modeling and observations. The IOEB data indicate, however, that mixing events reaching the halocline, and even the thermocline deeper down, did occur in different areas of the Arctic. How do we reconcile this apparent contradiction?

[34] In our opinion, the result here complements the prevailing view about the Arctic halocline. Salinity in the Arctic mixed layer from the IOEB data was about 1 psu lower than that of the halocline water, even during winter. This indicates that the water column was always statically stable, consistent with the widely held view that brine rejection is not sufficient to destabilize the upper water column. The forcing mechanism responsible for the IOEB-observed mixing events was not static instability induced by brine rejection, but an enhanced kinetic energy input associated with storm activity. Brine rejection, however, may have augmented the mixing in winter.

[35] In summary, we have used data from IOEBs in various regions of the Arctic Ocean to study mixing events which penetrated the halocline layer. All the mixing events were mechanically driven by intense storms. The IOEB-observed mixing occurred both in spring (when ice was melting) and in winter (when ice cover was maximum), as well as in areas with very different hydrographic structure.

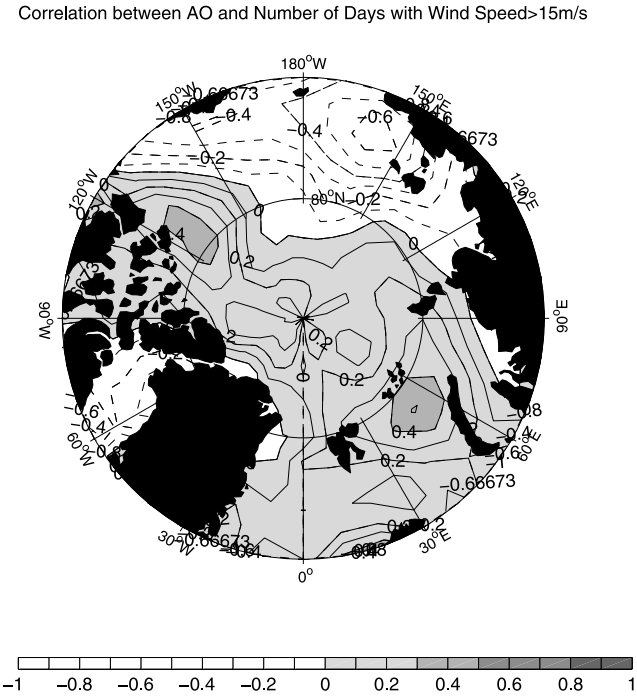

Figure 23. The correlation between stormy days and the AO index for the period between 1945 and 2000. Here we used the NCEP-NCAR reanalysis data for the surface wind. A day is defined to be "stormy" when the daily average surface wind is stronger than 15 m s^{-1}.

Thus it is plausible that storm-driven mixing occurs commonly over the whole Arctic Ocean. Further, IOEBs may not be located in the center of the storm areas. It is likely that mixing could have reached deeper depths in areas with stronger winds. How much does storm-driven mixing affect the overall heat and salt budget of the Arctic Ocean mixed layer, and how does it affect the atmosphere-ocean-ice interaction there? To answer these questions we need many more observations, as well as models capable of simulating oceanic responses to both synoptic and longer timescale atmospheric forcing.

[36] **Acknowledgments.** This study has been supported by the NASA Cryospheric Science Program and the International Arctic Reseach Center. We benefited from discussion with Dr. A. Proshutinsky. D. Walsh wishes to thank the Frontier Research System for Global Change for their support. The IOEB program was supported by ONR High-Latitude Dynamics Program and Japan Marine Science and Technology Center (JAMSTEC). Woods Hole Oceanographic Institution contribution number 11071.

References

Aagaard, K., L. K. Coachman, and E. Carmack (1981), On the halocline of the Arctic Ocean, *Deep Sea Res., Part A*, *28*, 529–545.

Carmack, E. C., et al. (1997), Changes in temperature and tracer distributions within the Arctic Ocean: Results from 1994 Arctic Ocean section, *Deep Sea Res., Part II*, *44*, 1487–1502.

Colony, R., and A. S. Thorndike (1984), An estimate of the mean field of sea ice motion, *J. Geophys. Res.*, *99*, 10,623–10,629.

Comiso, J. C. (1995), Remote sensing of the Arctic, in *Arctic Oceanography: Marginal Ice Zones and Continental Shelves*, *Coastal Estuarine Stud.*, vol. 48, edited by W. Smith and J. Grebmeier, pp. 1–50, AGU, Washington, D. C.

Dickson, R. R., J. Meincke, S. A. Malmberg, and A. J. Lee (1988), The "Great Salinity Anomaly" in the northern North Atlantic 1968–1982, *Prog. Oceanogr.*, *20*, 103–151.

Honjo, S., T. Takizawa, R. Krishfield, J. Kemp, and K. Hatakeyama (1995), Discoveries about interactive processes in the Arctic Ocean, *Eos Trans. AGU*, *76*, 209–219.

Kalnay, E., et al. (1996), The NCEP/NCAR 40-year Reanalysis Project, *Bull. Am. Meteorol. Soc.*, *77*, 437–472.

Krishfield, R., K. Doherty, and S. Honjo (1993), Ice-Ocean Environmental Buoys (IOEB); Technology and deployment in 1991–1992, *WHOI Tech. Rep. 93-45*, 138 pp., Woods Hole, Mass.

Krishfield, R., S. Honjo, T. Takizawa, and K. Hatakeyama (1999), Ice-Ocean Environmental Buoy Program: Archived data processing and graphic results from April 1992 through November 1998, *WHOI Tech. Rep. 99-12*, 83 pp., Woods Hole, Mass.

Kwok, R. (2000), Recent changes in the Arctic Ocean sea ice motion associated with the North Atlantic Oscillation, *Geophys. Res. Lett.*, *27*, 775–778.

Kwok, R., and D. Rothrock (1999), Variability of Fram Strait ice flux and North Atlantic Oscillation, *J. Geophys. Res.*, *104*, 5177–5188.

Maykut, G. A., and M. G. McPhee (1995), Solar heating of the arctic mixed layer, *J. Geophys. Res.*, *100*, 24,691–24,703.

Moore, R. M., and D. W. R. Wallace (1988), A relationship between heat transfer to sea ice and temperature-salinity properties of Arctic Ocean waters, *J. Geophys. Res.*, *93*, 565–571.

Morison, J. H., K. Aagaard, and M. Steele (2000), Recent environmental changes in the Arctic: A review, *Arctic*, *53*, 359–371.

Mysak, L. A., and S. A. Venegas (1998), Decadal climate oscillations in the Arctic: A new feedback loop for atmosphere-ice-ocean interactions, *Geophys. Res. Lett.*, *25*, 3067–3610.

Mysak, L. A., D. K. Manak, and R. F. Marsden (1990), Sea-ice anomalies observed in the Greenland and Labrador Seas during 1901–1984 and their relation to an interdecadal Arctic climate cycle, *Clim. Dyn.*, *5*, 111–133.

Parkinson, C. L., D. J. Cavalieri, H. J. Zwally, and J. C. Comiso (1999), Arctic sea ice extents, areas, and trends, 1978–1996, *J. Geophys. Res.*, *104*, 20,837–20,856.

Polyakov, I. V., A. Y. Proshutinsky, and M. A. Johnson (1999), Seasonal cycles in two regimes of Arctic climate, *J. Geophys. Res.*, *104*, 25,761–25,788.

Power, S. B., and L. A. Mysak (1992), On the interannual variability of Arctic sea-level pressure and sea ice, *Atmos. Ocean*, *30*, 551–577.

Proshutinsky, A. Y., and M. A. Johnson (1997), Two circulation regimes of the wind-driven Arctic Ocean, *J. Geophys. Res.*, *102*, 12,493–12,514.

Serreze, M. C., and R. Barry (1988), Synoptic activity in the Arctic Basin, 1979–85, *J. Clim.*, *1*, 1276–1295.

Slonosky, V. C., L. A. Mysak, and J. Derome (1997), Linking Arctic sea-ice and atmosphere circulation anomalies on interannual and decadal timescales, *Atmos. Ocean*, *35*, 333–366.

Steele, M., and T. Boyd (1998), Retreat of the cold halocline layer in the Arctic Ocean, *J. Geophys. Res.*, *103*, 10,419–10,435.

Steele, M., and J. H. Morison (1993), Hydrography and vertical fluxes of heat and salt northeast of Svalbard, *J. Geophys. Res.*, *98*, 10,013–10,024.

Thompson, D. W. J., and J. M. Wallace (1999), The Arctic Oscillation signature in the wintertime geopotential height and temperature fields, *Geophys. Res. Lett.*, *25*, 1297–1300.

Thorndike, A. S., and R. Colony (1980), Arctic Ocean Buoy Program data report, 19 January–31 December 1979, 131 pp., Polar Sci. Cent., Appl. Phys. Lab., Univ. of Wash., Seattle.

Thorndike, A. S., and R. Colony (1982), Sea ice motion in response to geostrophic winds, *J. Geophys. Res.*, *87*, 5845–5852.

Walsh, J. E., W. L. Chapman, and T. L. Shy (1996), Recent decrease of sea level pressure in the central Arctic, *J. Clim.*, *9*, 480–486.

Yang, J., J. Comiso, R. Krishfield, and S. Honjo (2001), Synoptic storms and the development of the 1997 warming and freshening event in the Beaufort Sea, *Geophys. Res. Lett.*, *28*, 799–802.

J. Comiso, Laboratory for Hydrospheric Processes, Code 971, NASA Goddard Space Flight Center, Greenbelt, MD 20771, USA.

S. Honjo and R. Krishfield, Department of Geology and Geophysics, Woods Hole Oceanographic Institution, Woods Hole, MA 02543, USA.

D. Walsh, International Arctic Research Center, University of Alaska, Fairbanks, Fairbanks, AK 99775, USA.

J. Yang, Department of Physical Oceanography, Woods Hole Oceanographic Institution, Woods Hole, MA 02543, USA. (jyang@whoi.edu)